

# Production of glass spheres from blast furnace slags by a thermal flame projection process

E.M. Saucedo-Salazar<sup>a,\*</sup>, Y.A. Perera-Mercado<sup>a</sup>, F.R. Rodríguez-Ruiz<sup>a</sup>, A. Arauza-Villarreal<sup>b</sup>

<sup>a</sup>*Centro de Investigación en Química Aplicada, Boulevard Enrique Reyna No. 140, C.P. 25294 Saltillo, Coahuila, México*

<sup>b</sup>*Altos Hornos de México S.A.B., Prolongación Juárez S/N, C.P. 25770 Monclova, Coahuila, México*

Received 2 April 2013; accepted 1 July 2013

Available online 16 July 2013

## Abstract

Blast furnace slags (BFS) were transformed into glass porous spheres by applying a natural gas/oxygen thermal projection process. Three types of BFS were selected as a function of their age or storage time. Effect of type of precursor, as well as gases mixture, feeding distance and feeding rate on density, morphology, microstructure and particles size of generated spheres were evaluated. It was found that despite of the slag age, obtained spheres are completely amorphous, and that the feeding distance has an important effect on spheres densities. Optimum treatment conditions were established in order to generate glass porous spheres with lower densities than their precursors.

© 2013 Elsevier Ltd and Techna Group S.r.l. All rights reserved.

**Keywords:** B. Microstructure—final; Thermal treatment; Density; Blast furnace slag

## 1. Introduction

Nowadays a lot of researches are aimed to reuse industrial byproducts in order to preserve natural resources used as raw materials and generating new materials with novel applications from these byproducts. All over the world, steel industry generates huge quantities of byproduct such as slags, residual waters, etc. In particular, blast furnace slags (BFS) have been used in construction industry in special formulations due to their properties such as high resistance and hardness, fire resistance and thermal insulator, but only a little percentage of slags are reused, and the rest are confined in dedicated places. BFS are mostly crystalline, and therefore, their hydraulic properties are low, which affect their behavior in cement formulations. In this work, BFS were treated by means of a thermal flame assisted process in order to obtain porous glass spheres with the lowest possible density that could show an improved behavior as thermal and acoustic insulators for building construction systems or even that can be used as lightening agents in cement formulations.

Chemical composition of BFS mainly depends of the iron ore composition used as raw material, beside other components; in general terms the main constituents are calcium oxide (CaO), Silicon (SiO<sub>2</sub>), Alumina (Al<sub>2</sub>O<sub>3</sub>) and magnesium oxide (MgO) compounds, which are also the main components of Portland cement [1–5], therefore high quantities of these compounds in a slag would improve its cementing properties [6].

About slag crystallinity, it depends on its solidification rate. When it is too fast, the obtained slag is mostly glass, but if the cooling process is slow, the structure could be crystalline where the following phases can be found: gehlenite (Ca<sub>2</sub>Al<sub>2</sub>SiO<sub>7</sub>), aquermanite (Ca<sub>2</sub>MgSi<sub>2</sub>O<sub>7</sub>), merwinite (Ca<sub>3</sub>MgSi<sub>2</sub>O<sub>8</sub>), bredigite (Ca<sub>14</sub>Mg<sub>2</sub>(SiO<sub>4</sub>)<sub>8</sub>), di-calcium silicate (Ca<sub>2</sub>SiO<sub>4</sub>) and others [5].

On the other hand, ceramics spheres are inorganic materials finely dispersed which can show a glassy, crystalline or glass-ceramic structure [7–16]. Övecoglu [17] has carried out the microstructural characterization of slag-based glass ceramics obtained by melting and crystallization at 950° and 1100 °C in order to determine the optimal conditions to generate glass ceramics for cladding and tiling applications. It was found that grain size, as well as wear, hardness, fracture toughness of these glass ceramics are affected by the presence of a nucleant agent. Also, Francis [18] have been aimed to study the crystallization behavior of BFS exposed to thermal treatments to obtain glass ceramics products, founding that conversion of

\*Corresponding author. Tel.: +52 844 4 38 98 30; fax: +52 844 4 38 98 39.

E-mail addresses: [esmeralda.saucedo@ciqua.edu.mx](mailto:esmeralda.saucedo@ciqua.edu.mx),  
[esmesaucedo@hotmail.com](mailto:esmesaucedo@hotmail.com), [esaucedo@ciqua.mx](mailto:esaucedo@ciqua.mx) (E.M. Saucedo-Salazar).

BFS could be an alternative to produce glass ceramic materials. More recently, studies to clarify the phase separation mechanism of BFS have been carried out by Karamberi [19] and it was found that it depends on BFS composition and heat treatment conditions since controlled crystallization is related to the separation of a crystalline phase from the glassy parent phase to form tiny crystals. Finally, Saucedo [20] has demonstrated that it is possible to transform BFS into glass ceramic spheres by applying a thermal plasma process. From these works, it is thought that a thermal flame treatment could be a cheaper alternative to transform BFS. In a thermal flame treatment, a blend of oxygen and natural gas is projected through a flame gun to form a plume; once the plume is formed, powdered precursor is injected near to the nozzle and then, it is projected through the flame. Inside the flame, precursor particles can reach high enough temperatures to be chemical, structural and morphologically transformed.

## 2. Experimental

To carry out this work a commercial flame gun was used. A blend of oxygen and natural gas was used to form the flame. These gases are injected through the nozzle; once the flame is formed, powdered precursors are injected near to the nozzle and then, they are projected through the flame. After this treatment, the projected particles are trapped and cooled in a special recollection device.

Three types of blast furnace slags were selected according to their storage time. Young (storage time < 1 year), middle age (storage time: 5–10 years), and old (storage time > 20 year) slags were considered. All slags were pretreated following a mineralogical processing to prepare them for the thermal transformation process. This pretreating process includes: crushing, drying, grinding and sieving. For all precursors, a particle size between 106 and 150  $\mu\text{m}$  was selected to be used in this work.

Several parameters, such as oxygen and natural gas feeding rates, and feeding distance were evaluated in order to establish the optimal experimental conditions to generate hollow and/or porous spheres which would be related to reduction of spheres densities in comparison to their precursors. Table 1 summarizes the used parameters to form the flame. During all treatments, oxygen and natural gas pressure was maintained at 10 psi. About the flame, other parameter is the crown length, which is referred to the internal and most intense part of the flame and depends on the oxygen and natural gas feeding rates into the nozzle. Fig. 1 shows examples of measurements of crown length. Feeding distance is referred to the length from the nozzle to the precursor feeding point, see Fig. 2.

On the other hand, real density measured by helium picnometry, was used as indicator to establish the optimal projection parameters

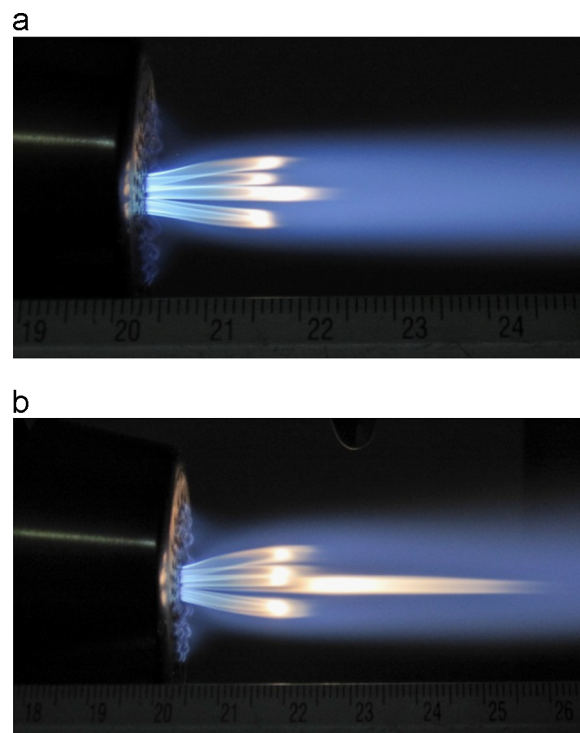


Fig. 1. Crown length of the flame: (a) 2 cm and (b) 6 cm.

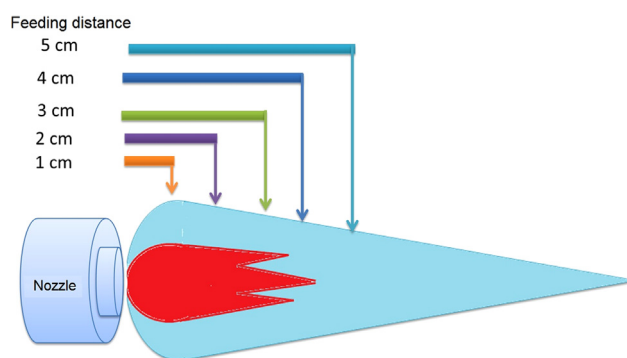


Fig. 2. Measurements of the precursor feeding distance into the flame.

for the three evaluated slags, which were the following: gas natural flux: < 1 L/min; oxygen flux: 6 L/min, which leads to a crown length of 6 cm. Also morphological and structural characterization was carried out on the particles obtained under these optimal operation parameters, as well on the three precursors.

### 2.1. Morphology and particle size

Spherical particles obtained from the projection process were observed using an optical microscope Olympus model BX60. These particles were observed using transmitted light and bright field at 50 $\times$  and 100 $\times$  magnifications.

Morphology of slags and spheres were evaluated by scanning electron microscopy using a microscope FEI Quanta 3D in low vacuum mode. Elemental analysis for each sample was also obtained by X-ray dispersive energy spectroscopy (EDS) using a microscope TOP-CON SM 510.

Table 1

Parameters used in the projection process.

Oxygen flow (L/min)	6, 6.5, 7, 7.5, 8, 9
Natural gas flow (L/min)	1, < 1
Feeding distance (cm)	1, 2, 3, 4, 5

## 2.2. Microstructure and phase identification

In order to identify the slags crystalline phases as well as of the obtained spheres, a X-ray diffractometer Siemens 500 was used, under the following conditions: radiation Cu K $\alpha$  ( $\lambda = 1.5418 \text{ \AA}$ ) at 35 kW and 25 mA, in a  $2\theta$  range from  $5^\circ$  to  $70^\circ$ .

## 2.3. Real density

Real density and real volume of slags and spheres were obtained using a helium picnometer AccuPyc II 1340. Tests were carried out according to standard ASTM D5965.

## 2.4. Chemical composition

Content of  $\text{Al}_2\text{O}_3$ ,  $\text{MgO}$ ,  $\text{Mn}$ ,  $\text{Fe}$ ,  $\text{Na}_2\text{O}$ ,  $\text{K}_2\text{O}$ ,  $\text{Zn}$ ,  $\text{TiO}_2$  was determined using spectrometer Perkin Elmer model Analyst 700. Carbon and sulfur were determined by simultaneous determination using a detector Leco CS600; and  $\text{SiO}_2$  and  $\text{CaO}$  by wet methods.

## 3. Results and discussion

### 3.1. Morphology

All of the three evaluated BFS precursors, despite of their age and storage time, are constituted by particles with irregular shapes and sizes. Elemental analyses obtained by EDS show evidence of the following elements: silicon, calcium, aluminum and magnesium; and in lower proportion, manganese, iron, sodium, potassium and sulfur. Fig. 3 shows the morphology and X-ray spectra of the young BFS (< 1 year).

About the transformed particles, Fig. 4 shows optical micrographs at  $50\times$  and  $100\times$  of spheres generated from the young slag (< 1 year). These results show mainly two effects of the treatment: firstly, that all of the projected particles have been completely transformed into spheres; and, that these spheres are translucent, allowing to observe inside of them, giving the first indication that these materials are vitreous. These effects are observed for all cases independently of the used precursor.

By scanning electron microscopy the spherical shapes of the transformed particles is corroborated, and also, porosity is observed in the surface of some spheres, see Fig. 5. Average diameter for each system was calculated by measuring the diameter in at least 50 particles of each system. The obtained values are the following: 122.05, 115.51 and 120.22  $\mu\text{m}$ , for the spheres obtained from the young, middle age and old slags respectively.

### 3.2. Microstructure

Fig. 6 shows BFS X-diffraction patterns. As can be observed, the three selected slags are completely crystalline. The following phases were identified: akermanite ( $\text{Ca}_2\text{MgSi}_2\text{O}_7$ ), gehlenite ( $\text{Ca}_2\text{Al}_2\text{SiO}_7$ ), and merwinite ( $\text{Ca}_3\text{MgSi}_2\text{O}_8$ ). Others low intensity peaks were observed which could be indexed as bredigite

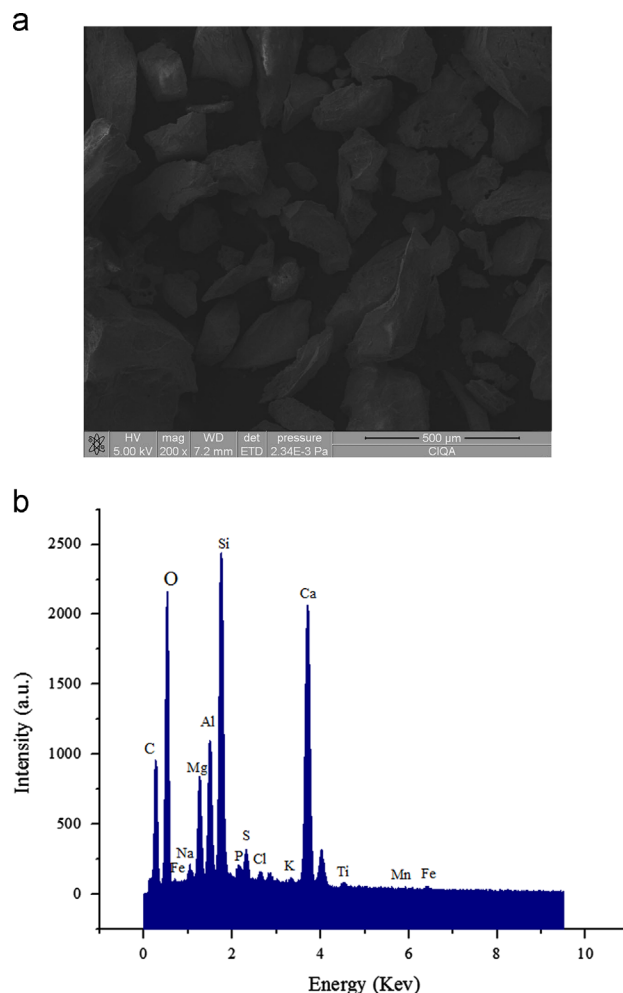


Fig. 3. (a) Morphology (SEM image) and (b) qualitative analysis (EDS spectrum) of the youngest slag (BFS < 1 year).

( $\text{Ca}_{14}\text{Mg}_2(\text{SiO}_4)_8$ ), as an additional crystalline phase. This phase is a double calcium–magnesium silicate that appears due to the production and cooling slag kinetics.

Fig. 7 shows diffractograms for the spheres obtained from the three precursors. For all the evaluated systems, independently of their age, there is no evidence of crystalline phases, only a dome around  $2\theta = 30^\circ$  is observed, which indicates that the spheres have an amorphous structure [21].

### 3.3. Chemical composition of BFS and spheres

Table 2 shows chemical composition of BFS and obtained spheres for all the systems. All the slags are in the permissible ranges for BFS [1,5,6]. As can be observed in the slags composition, sulfur content is higher in the young slags, than in the middle age and in the old slags. For the obtained spheres, it is worth to note that for all cases, the sulfur content diminishes, as well as the content of other compounds such as  $\text{K}_2\text{O}$  and  $\text{Na}_2\text{O}$ , is also decreased in comparison to their precursors. It is thought that, as well that in plasma treatment, a chemical decomposition takes place during spheroidization process generating gases such as  $\text{SO}_3$  gas, in the case of sulfur compounds, which are released from the spheres causing the



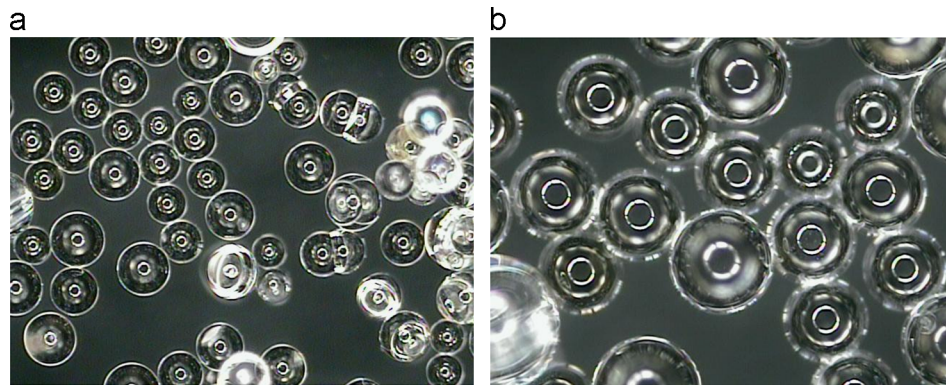


Fig. 4. Morphology of projected particles from the youngest slags at (a) 50  $\times$  and (b) 100  $\times$ .

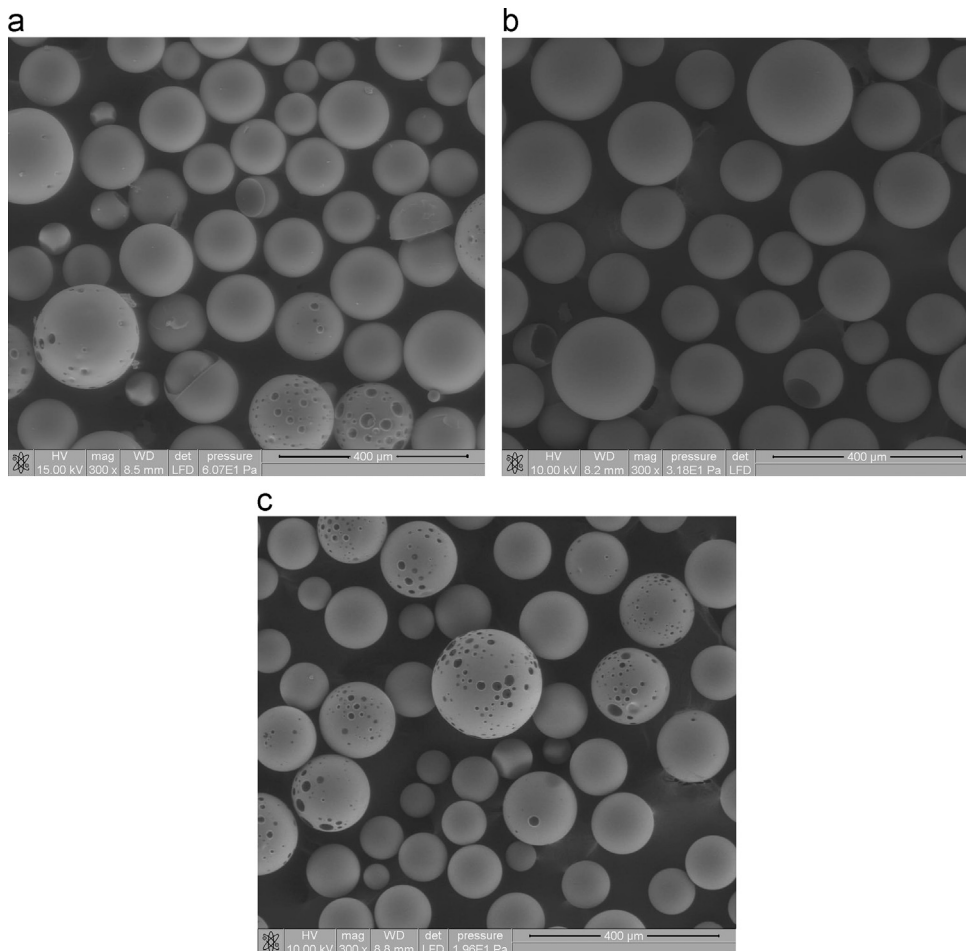


Fig. 5. Morphology and superficial porosity of spheres obtained from (a) youngest (< 1 year) (b) middle age (5–10 years) and (c) oldest slags (> 20 years).

porosity observed by electron microscopy, and therefore a reduction in density values [20].

When precursor particles with angular geometries are fed into the plume, they can reach high enough temperatures to be softened or even melted, besides a chemical decomposition and changes in crystalline structure take place. These changes in chemical composition lead to bubbles generation due to the decomposition of certain compounds meanwhile these particles adopt a spherical morphology, generating mainly porous

spheres. If these spheres are kept at high temperatures, gases are completely released from them and the spheres begin to collapse resulting in the formation of solid spheres depending on the residence time of the particle inside the plume. This mechanism can vary depending on the composition of each particle and reached temperature is related to the material viscosity. This mechanism was previously proposed for BFS transformation process using an Ar–He plasma plume [20]. According to the obtained results in this work, it is thought that

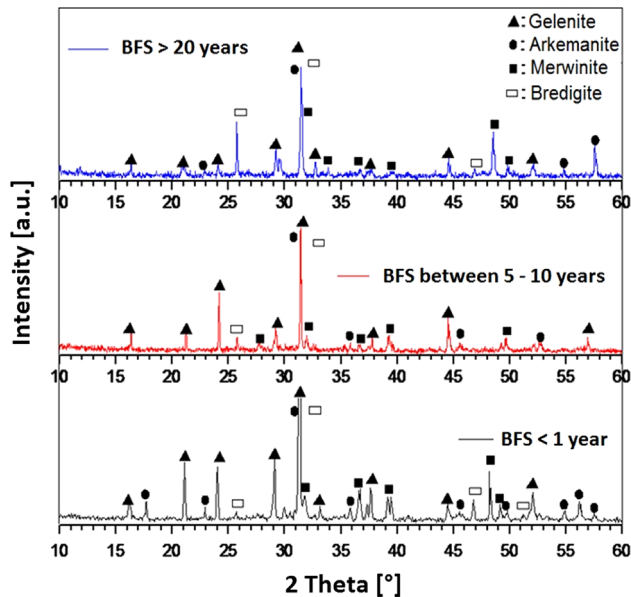


Fig. 6. X-Ray diffraction patterns of the three kinds of blast furnace slags.

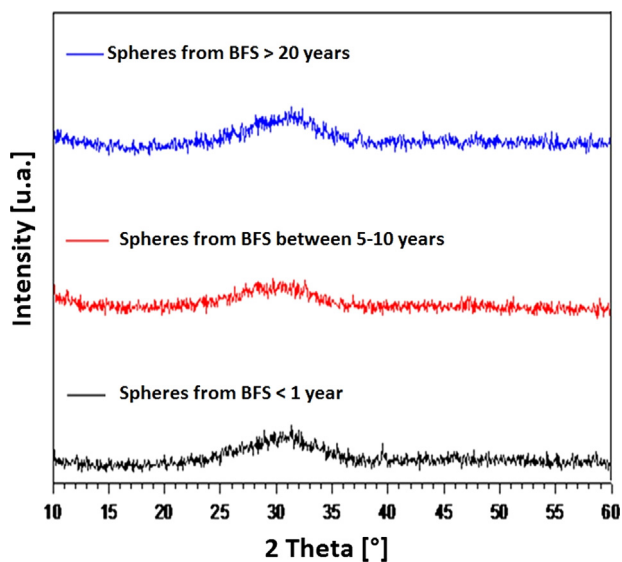


Fig. 7. X-ray diffraction patterns of spheres.

a similar mechanism take place when a gas/oxygen plume is used in the same kind of precursors.

### 3.4. Real density of BFS and vitreous spheres

Real density values of precursors and spheres are shown in Table 3. For precursors, density values are in the range between 2.95 and 2.98 g/cm<sup>3</sup>. As can be observed, middle age BFS (5–10 years) are the ones that show the highest density value, which could be due to the increase in titanium oxide content observed in this slag.

On the other hand, once that the optimum projection parameters for density reduction of the spheres were established, the effect of precursors feeding distance into the plume was studied. Fig. 8 shows the density variation of spheres

Table 2

Chemical composition of BFS and spheres.

Compound	BFS			Spheres		
	< 1 year	5–10 years	> 20 years	< 1 year	5–10 years	> 20 years
SiO <sub>2</sub>	38.4	39.9	33	39.9	40.2	35.4
Al <sub>2</sub> O <sub>3</sub>	12.98	13.63	12.25	13.19	13.84	13.26
CaO	34.8	32.4	32.7	34.8	33.9	34.2
MgO	8.58	7.75	9.405	8.7	8	10.0
TiO <sub>2</sub>	3.42	4.9	1.59	3.27	5.01	1.76
K <sub>2</sub> O	0.837	0.855	0.385	0.24	0.316	0.268
Na <sub>2</sub> O	0.802	0.539	0.205	0.29	0.296	0.256
S	1.26	0.99	1.21	0.09	0.04	0.099
P	0.124	0.041	0.08	0.069	0.072	0.066
Mn	0.48	0.64	0.45	0.49	0.65	0.48
C	0.076	0.11	1.32	0.05	0.037	0.57
Fe	0.48	0.46	0.45	0.44	0.43	0.48

Table 3

Spheres average diameter, spheres density, precursor density, and density reduction of spheres.

	Spheres (< 1 year)	Spheres (5–10 years)	Spheres (> 20 years)
Average diameter (μm)	122.05	115.51	120.22
BFS density (g/cm <sup>3</sup> )	2.97	2.98	2.95
Spheres density (g/cm <sup>3</sup> )	2.49	2.65	2.61
Density reduction (%)	16	11	12

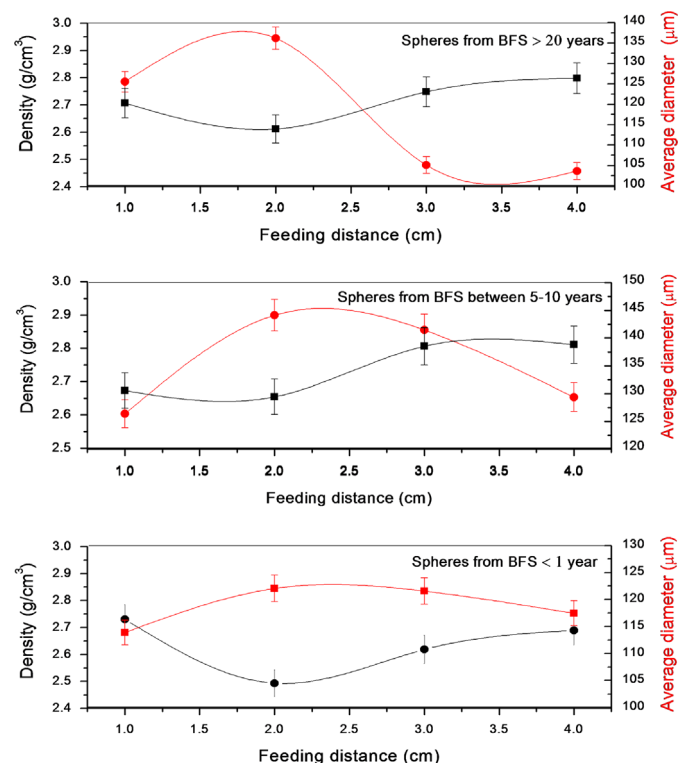


Fig. 8. Average diameters and density variation of spheres as a function of precursor feeding distance.

generated at different feeding distances for the three precursors. At 2 cm of feeding distance, a remarkable density

reduction for the three systems is observed. Also for the three systems, is observed that up to 2 cm of feeding distance, the densities are increased, which could be attributed to the fact that during the gas expansion step inside the spheres; once that these gases are expelled from the spheres, they tend to reduce their size and increase their densities.

As can be observed in Table 2, spheres generated from the young BFS (< 1 year) have the highest average diameter, and also show the lowest density, and therefore it is expected to have the major quantity of porous spheres. Middle age slags (5–10 years) show the lowest average diameter and also has the highest density. Finally, BFS > 20 years has intermediate values of diameter and density.

In a previous work [20], a reduction of 7% in density from BFS precursor was reported using an Ar–He plasma treatment of slags. For this work, and using three kinds of precursors, higher density reduction percentages, up to 16% for the young BFS were obtained. This system also contains the highest quantity of sulfur, potassium and sodium oxides in its composition. For the other systems studied a reduction in densities also is observed between 11% and 12%.

#### 4. Conclusions

Vitreous spheres were synthesized from three kind of crystalline BFS used as precursors applying a gas/oxygen flame projection process. Optimal parameters to obtain the highest quantity of spheres with lower density than their precursors were established: natural gas flux < 1 L/min; oxygen flux of 6 L/min and feeding distance of 2 cm. The highest density reduction (16%) was observed for the young BFS (< 1 year). Generation of porous or dense spheres could be controlled by adjusting the thermal process parameters.

#### Acknowledgment

This work was supported by the FOMIX Coahuila Funds through Grant no. COAH-2010-C14-149386. Authors acknowledge to S.P. García, B. Huerta, M. Lozano, J.A. Cepeda and M.A. Cenicerós for their technical support.

#### References

[1] R. Montalvo, E. Zeballos, P. Paz, J. Huayna, M. Casaverde, Slags characterization by X-ray diffraction, *Elementos: Ciencia y Cultura* 13 (2006) 61–63.

[2] J.I. Escalante-García, J. Méndez-Nonell, A. Gorokhovskiy, P.E. Fraire-Luna, H. Mancha-Molinari, G. Mendoza-Suarez, Reactividad y propiedades mecánicas de escoria de alto horno activada por álcalis, *Boletín de la Sociedad Española Cerámica y Vidrio* 41 (2002) 451–458.

[3] L. Espinoza, I. Escalante, Comparación de las propiedades del concreto utilizando escoria de alto horno como reemplazo parcial y total del cemento Portland ordinario, *Nexo* 21 (2008) 11–18.

[4] ASTM C 125, Standard Terminology Relating to Concrete and Concrete aggregates, American Society for Testing and Materials (ASTM), West Conshohocken, PA, 1998.

[5] L.L. Amaral, Hormigones con escorias de horno eléctrico como áridos: propiedades durabilidad y comportamiento ambiental (Ph.D. Thesis), Universidad Politécnica de Cataluña (1999).

[6] S.C. Pal, A. Mukherjee, S.R. Pathak, Investigation of hydraulic activity of ground granulated blast furnace slag in concrete, *Cement and Concrete Research* 33 (2003) 1481–1486.

[7] V.V. Budov, Hollow glass microspheres: use, properties, and technology (Review), *Glass and Ceramics* 51 (7–8) (1994) 230–235.

[8] L.Y. Novoselova, E.E. Sirotkina, N.I. Pogadaeva, I.V. Russkikh, Aluminosilicate microspheres in fly ashes from thermal power plants and their use for the removal of petroleum and phenol from water, *Solid Fuel Chemistry* 42 (3) (2008) 177–182.

[9] E.F. Medvedev, Hydrogen permeability of microspheres based on ash and slag, *Science for Ceramic Production* 59 (2002) 374–377.

[10] V.S. Bessmertnyi, V.P. Krokhin, A.A. Lyashko, N.A. Drizhd, Zh. E. Shekhovtsova, Production of glass microspheres using the plasma-spraying method, *Glass and Ceramics* 58 (8) (2001) 6–7.

[11] M.S. Allen, R.G. Baumgartner, J.E. Fesmire, S.D. Augusty Nowicz, Advances in microsphere insulation systems, in: *Proceedings of the Cryogenic Engineering Conference* (2003).

[12] J.-H. Im, J.-H. Lee, D.-W. Park, Synthesis of nano-sized tin oxide powder by argon plasma jet at atmospheric pressure, *Surface and Coatings Technology* 202 (2008) 5471–5475.

[13] S. Ruixue, L. Yupeng, C. Kezheng, Preparation and characterization of hollow hydroxyapatite microspheres by spray drying method, *Materials Science and Engineering* 29 (2009) 1088–1099.

[14] H.F.W. Taylor, in: *Cement Chemistry*, Second edition, Academic Press, London, UK, 2004.

[15] P.C. Hewlett, *Lea's Chemistry of Cement and Concrete*, Elsevier, Great Britain, 1998.

[16] J. Zarzycki, *Glasses and the Vitreous State*, Cambridge University Press, Great Britain, (1991), 37–74, 148–183, 334–347.

[17] M.L. Övecoglu, Microstructural characterization and physical properties of a slag-based glass-ceramic crystallized at 950 and 100 °C, *Journal of the European Ceramic Society* 18 (1998) 161–168.

[18] A. Francis, Conversion of blast furnace slag into new glass-ceramic material, *Journal of the European Ceramic Society* 24 (2004) 2819–2824.

[19] A. Karamberi, K. Orkopoulos, A. Moutsatsou, Synthesis of glass-ceramics using glass cullet and vitrified industrial by products, *Journal of the European Ceramic Society* 27 (2007) 629–636.

[20] E.M. Saucedo, Y.A. Perera, D. Robles, *Ceramics International Journal* 38 (2012) 3161–3165.

[21] Y. Li, X. Liu, H. Sun, D. Cang, Mechanism of phase separation in BFS (blast furnace slag) glass phase, *Science China Technological Sciences* 54 (2011) 105–109.